PROCEEDINGS OF THE 8TH INTERNATIONAL CONFERENCE ON DISCRETE ELEMENT METHODS (DEM8)

A MICROMECHANICAL, μUNSAT, APPROACH FOR WET GRANULAR SOILS

Jérôme Duriez[1], Sacha Duverger[2] and Richard Wan[3]

[1] Irstea, Aix Marseille Univ, RECOVER
3275 route Cézanne, CS 40061, 13182 Aix-en-Provence Cedex 5, France
jerome.duriez@irstea.fr http://www.irstea.fr/duriez

[2] Irstea, Aix Marseille Univ, RECOVER
3275 route Cézanne, CS 40061, 13182 Aix-en-Provence Cedex 5, France
sacha.duverger@irstea.fr

[3] Dept of Civil Engineering, University of Calgary
2500 University Dr NW, Calgary, Alberta T2N 1N4, Canada
wan@ucalgary.ca http://people.ucalgary.ca/∼wan/

Keywords Unsaturated Soils, Effective Stress, μUNSAT approach

Abstract We herein present a recent micromechanical approach combining analytical homogenization with Discrete Element Method (DEM) simulations for a better understanding of the mechanical behavior of granular soils in an intermediate state of water saturation. Analytical homogenization first leads to a so-called μUNSAT general expression for the macroscopic stress state, starting from micro-scale internal forces. The μUNSAT equations involve surface tension in addition to capillary pressure, and show a tensorial nature in accordance with preferential directions for the internal forces at the micro-scale. A DEM approach then enables one to access all stress quantities in the specific case of ideal wet granular materials. The results discuss the stress-strain-strength effective nature of the contact stresses stemming from contact forces, as well as the tensorial, anisotropic, character of fluid-induced capillary stresses.

1 INTRODUCTION

Geotechnical operations most often face granular soils whose stiffness and strength are affected by a partial water saturation, as evidenced by the classical sandcastle example. In the long-lasting pursuit of an effective stress theory that would merge the mechanical behaviors in unsaturated (partially saturated) and dry, or saturated, conditions, experimental and numerical approaches [1, 2, 3, 4, 5, 6] have evidenced a possible unified description of stress limit states through the limit criterion pertaining to dry conditions. Such results were obtained dividing the macroscopic total stresses into two parts: first, so-called capillary stresses due to the air-water phases, completed by a second "effective" stress variable, being solid-phase related, which the dry limit criterion applies to regardless of saturation conditions. On the other hand, for what concerns the stress-strain behavior, constitutive relations for dry conditions could not be successfully applied to that same stress variable in order to describe the strains observed under partial saturation [3], except in a restricted domain of elastic behavior [7, 8, 9].

We thus herein synthetize recent results obtained in [5, 6, 10, 11, 8, 9] after a micro-mechanical approach combining analytical homogenization and Discrete Element Method (DEM) simulations. Analytical homogenization led to establish, after [12], a general expression, coined μUNSAT, for the stress state of unsaturated granular soils, which is first recalled in Section 2. Then, a DEM model extending [4] is proposed in Section 3 for ideal wet granular materials made of spherical particles and containing little water content in the forms of distinct meniscii, as per the pendular regime. DEM simulations finally enable one in Section 4 to measure and investigate all micro-scale stress quantities entering the μUNSAT expression.

2 μUNSAT ANALYTICAL HOMOGENIZATION OF AN UNSATURATED GRANULAR SOIL

We consider a granular soil whose solid phase s shows discrete particles p with sizes being in the order of $1/100^{\text{th}}$ to $1/10^{\text{th}}$ mm, i.e. a silt or a fine sand, for capillary effects to have a mechanical influence. While the solid phase occupies the volume $V_s = \cup_p V_p$, air and water phases respectively occupy V_a and V_w volumes, with $V = V_s \cup V_a \cup V_w$ being the total volume. We denote S_r the saturation ratio $V_w/(V_w + V_a)$. The total stresses are then expressed in Eq. (1) as the macroscopic average of micro-scale stresses in the different phases, including the air-water interface S_{aw} which is prone to surface tension internal forces. In case fluid-solid surface tension would be significant as well, the corresponding interfaces could be considered in Eq. (1) without changing the subsequent developments, as soon as solid particles can be considered as rigid [11].

$$\boldsymbol{\Sigma} = \frac{1}{V}\left(\sum_{\alpha=a,s,w}\int_{V_\alpha}\boldsymbol{\sigma_\alpha}\,dV + \int_{S_{aw}}\boldsymbol{\pi}\,dS\right) \tag{1}$$

In terms of micro-scale internal forces, we denote $\boldsymbol{\sigma_\alpha} = u_\alpha\,\boldsymbol{\delta}$, $\alpha \in \{a, w\}$ the air and water pressures, $\vec{f}^c$ the contact forces between contacting solid particles whose centers form branch vectors $\vec{l}$, and γ the air-water surface tension. Algebraic manipulations then lead from Eq. (1) to the following μUNSAT stress expression [10, 11], assuming mechanical equilibrium for the particles:

$$\boldsymbol{\Sigma} - u_a\,\boldsymbol{\delta} = \boldsymbol{\sigma^{cont}} + \boldsymbol{\sigma^{cap}} \tag{2}$$

$$\boldsymbol{\sigma^{cont}} = \frac{1}{V}\sum_{cont.} \vec{f}^c \otimes \vec{l} \tag{3}$$

$$\begin{aligned}\boldsymbol{\sigma^{cap}} &= -\frac{1}{V}\left[u_c\left(V_w\,\boldsymbol{\delta} + \int_{S_{sw}} \vec{n}\otimes\vec{x}\;dS\right) + \gamma\left(\int_{S_{aw}} (\boldsymbol{\delta} - \vec{n}\otimes\vec{n})\;dS + \int_{\Gamma} \vec{\nu}\otimes\vec{x}\;dl\right)\right] \\ &= -\frac{1}{V}\left[u_c\left(\boldsymbol{\mu_{Vw}} + \boldsymbol{\mu_{Ssw}}\right) + \gamma\left(\boldsymbol{\mu_{Saw}} + \boldsymbol{\mu_{\Gamma}}\right)\right]\end{aligned} \tag{4}$$

Eq. (2) expresses the partition of the total (net) stresses between contact stresses $\boldsymbol{\sigma^{cont}}$ stemming from contact forces within the solid phase as per Eq. (3), and capillary stresses $\boldsymbol{\sigma^{cap}}$ due to the air-water mixture as per Eq. (4). The capillary stresses depend on the capillary pressure $u_c = u_a - u_w$ (corresponding to matric suction for granular soils), on surface tension γ, and on four microstructure tensors $\boldsymbol{\mu_{Vw}}$, $\boldsymbol{\mu_{Ssw}}$, $\boldsymbol{\mu_{Saw}}$, $\boldsymbol{\mu_{\Gamma}}$ pertaining to the water volume V_w, the wetted solid surfaces S_{sw}, the air-water interfaces S_{aw}, the contact lines Γ, and the orientations of those.

Two salient features can be distinguished in the μUNSAT expressions. They first include surface tension, being in this sense comparable to the thermodynamically inspired approaches of [13, 14], as opposed to [2, 3] where only capillary pressure enters the equations. The presence of air-water interfaces and corresponding surface tension is indeed understood as a distinct feature of triphasic (unsaturated) conditions, as opposed to biphasic (dry or saturated) ones. Second, the μUNSAT expressions endow, in (4), the fluid-induced capillary stresses with a clear tensorial nature in the general case. This clearly is in better agreeement with the material microstructure that includes for instance wetted solid surfaces experiencing water pressure along their normals only.

3 DEM MODELLING IN THE PENDULAR REGIME

Aiming to apply the μUNSAT expressions and investigate the capillary and contact stresses along loading paths, we now restrict ourselves to the case of spherical solid particles in binary interactions through distinct capillary bridges, in the so-called pendular saturation regime (Fig. 1). Under these conditions, DEM modelling is more than appropriate and we consider our DEM model proposed in [6], extending [4] to non-zero contact angles (θ in Fig. 1) and a more comprehensive description of air-water interfaces.

The model assumes uniform capillary pressure conditions, i.e. thermodynamic equilibrium, and computes in this case capillary bridges between particles pairs, solving the Laplace-Young equation [6]. The possibility and property of liquid bridges depend on considered u_c, θ, particle sizes and inter-particle distance. The model outputs a comprehensive description of the micro-scale, giving access to all microstructure tensors entering the μUNSAT equations, and to the macroscopic stress state as per the μUNSAT stress expressions (2)-(4), neglecting an uniform air pressure taken as reference. In the present

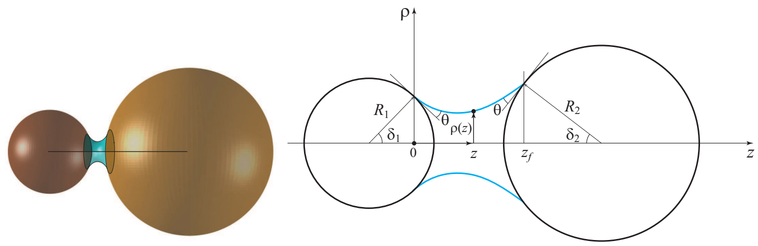

Figure 1: Capillary bridges in the pendular regime

pendular regime, Eqs. (2)-(4) are actually equivalent to the following, more classical, stress expression based on resultant forces [4]:

$$\boldsymbol{\Sigma} = \boldsymbol{\sigma^{cont}} + \frac{1}{V} \sum_{bridges} \vec{f}^{cap} \otimes \vec{l} \tag{5}$$

, obeying the virial theorem for discrete systems in binary interactions [15]. The equivalence between the force-based capillary stress expression in Eq. (5), and the μUNSAT one in Eq. (4), has indeed been demonstrated thanks to the Laplace-Young equation in [10, 11].

4 RESULTS AND DISCUSSION

Capillary and contact stresses are now analysed along strain-controlled loading paths which are axisymmetric around the '1' axis, with '2,3' the two other spatial directions, and defined by:

$$d\varepsilon_1 = cst \geq 0 \; ; \; d\varepsilon_2 = d\varepsilon_3 \; ; \; d\varepsilon_1 + 2\,R\,d\varepsilon_3 = 0 \tag{6}$$

, with R a constant for each loading path. While $R = 1$ corresponds to a constant-volume path, a fixed rate of contractancy (resp. dilatancy) is imposed for $R > 1$ (resp. $0 < R < 1$). By convention, the limit case $R = 0$ is chosen as contractant as well. The choice of such loading paths follows [8], and we refer to [6, 11, 16, 17, 9] for more classical triaxial loading paths. We choose $\boldsymbol{\varepsilon}$ as a monotonously increasing loading parameter, with

$$||\boldsymbol{\varepsilon}|| = \sqrt{{\varepsilon_1}^2 + 2\,{\varepsilon_3}^2} \tag{7}$$

, and describe all stress quantities $\boldsymbol{\Sigma}, \boldsymbol{\sigma^{cont}}, \boldsymbol{\sigma^{cap}}$ through the scalars p, q, p^{cont}, q^{cont}, p^{cap}, q^{cap} with e.g.

$$p = \frac{\Sigma_1 + 2\,\Sigma_3}{3} \tag{8}$$

$$q = \Sigma_1 - \Sigma_3 \tag{9}$$

Imposing the same strain paths on dense and loose packings in dry and wet conditions while measuring the response in terms of contact stresses, we aim to check whether a unique constitutive behavior links the strains $\boldsymbol{\varepsilon}$ to the contact stress $\boldsymbol{\sigma^{cont}}$ both in dry and wet conditions. Table 4 details the test conditions and the packing properties. Attention is paid to have dry/wet comparisons that are as close as possible in terms of initial contact stress states and initial properties for each dense or loose packings.

Table 1: Test conditions

	Dense packing		Loose packing	
	Dry	Wet	Dry	Wet
Initial p (kPa)	20.6	10	17.3	10
Imposed u_c (kPa)	—	125	—	125
Initial S_r (%)	—	0.85	—	0.50
Initial porosity (-)	0.370	0.373	0.436	0.438
Initial coordination number (-)	6.62	6.52	5.17	5.12

The results (Figs. 2 to 5) evidence that both the imposed dilatancy rate (R parameter) and the packing density affect the stress-strain effective character of the contact stress, in terms of the uniqueness of the behavior between dry and wet conditions. Good agreement is actually obtained between dry and wet contact stress responses in the case of contractant loading paths and for the dense packing. For less contractant loading paths, and/or a looser packing, dry and wet contact stress responses only agree in a limited initial regime. Further interpretation in terms of elastic or dissipative nature of these different regimes have been proposed in [8]. It is to note all contact stress paths are bounded by cohesionless Mohr-Coulomb lines determined for the two packings at hand in dry conditions in [16, 9], confirming the stress-strength effective nature of $\boldsymbol{\sigma^{cont}}$ already discussed in [6, 16, 9].

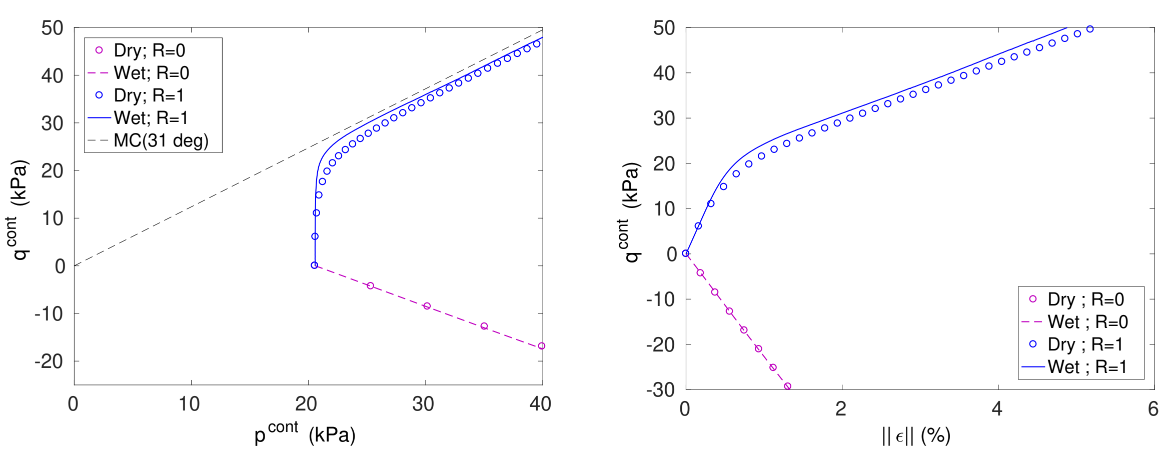

Figure 2: Dense packing: contact stress response along $R = 0$ (contractant) and $R = 1$ (isochoric) strain loading paths

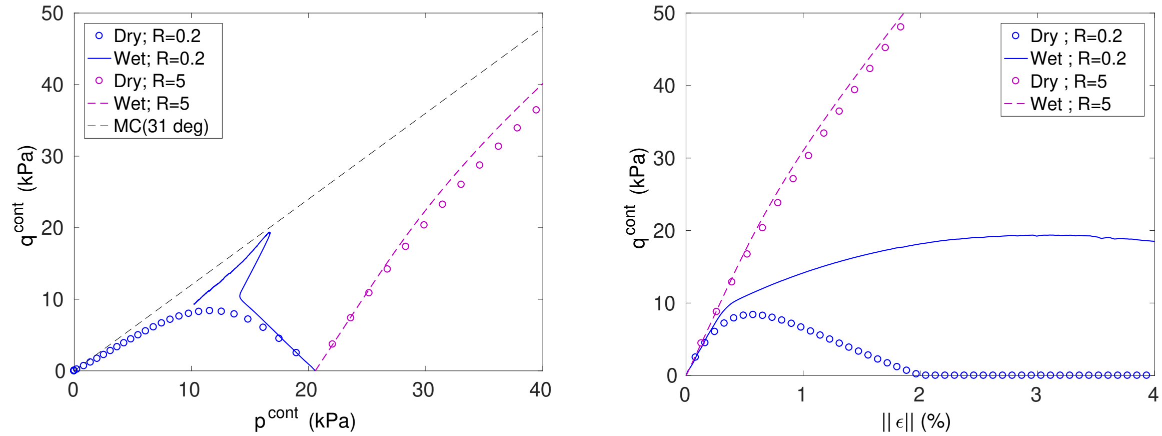

Figure 3: Dense packing: contact stress response along $R = 5$ (contractant) and $R = 0.2$ (dilatant) strain loading paths

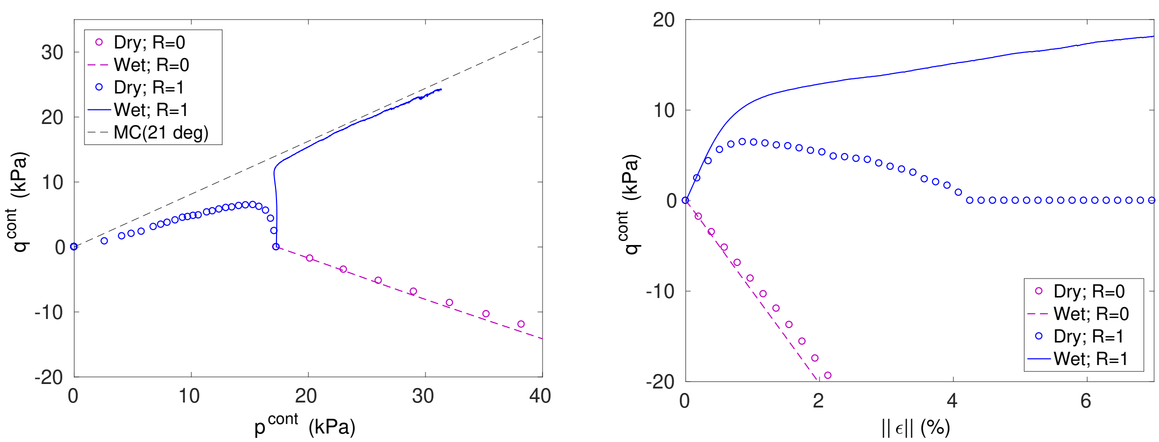

Figure 4: Loose packing: contact stress response along $R = 0$ (contractant) and $R = 1$ (isochoric) strain loading paths

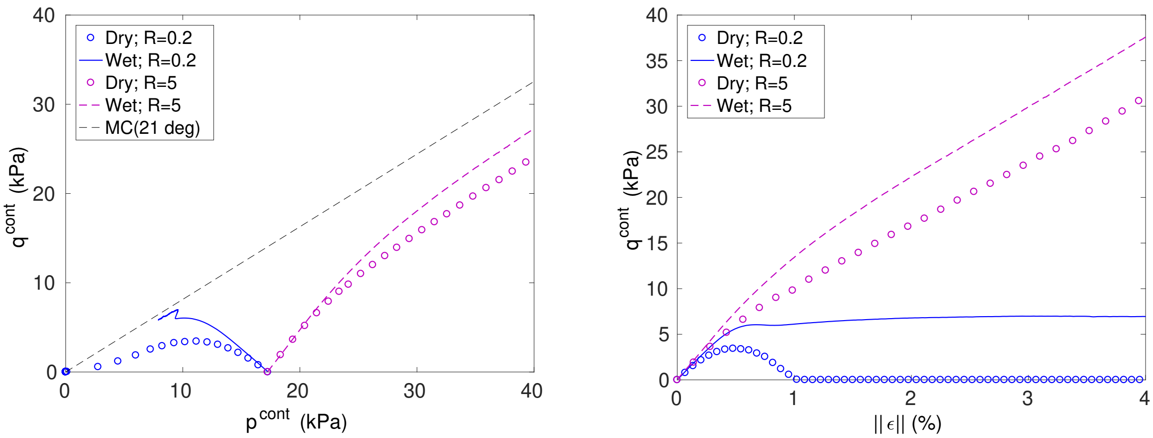

Figure 5: Loose packing: contact stress response along $R = 5$ (contractant) and $R = 0.2$ (dilatant) strain loading paths

As for the capillary stresses, their evolutions during the two loading paths $R = 1$ and $R = 5$ for the dense packing are illustrated in the Fig. 6. A non-negligible deviatoric component q^{cap} is obtained, in the order of 10-20% of the mean capillary stress p^{cap}, emphasizing how capillary stresses qualitatively deviate in the pendular regime from an average fluid pressure. Quantitatively, the Fig. 6 also considers Bishop's estimation of the capillary stresses [18], with $\chi = S_r$:

$$\boldsymbol{\sigma}^{\boldsymbol{cap}}_{\boldsymbol{Bish}} = -u_c\, S_r\, \boldsymbol{\delta} \tag{10}$$

The comparison with the μUNSAT approach shows how much Bishop's expression (10) underestimates the mean capillary stress in the pendular regime, in addition to missing out on the deviatoric component of $\boldsymbol{\sigma}^{\boldsymbol{cap}}$.

5 CONCLUSION AND PERSPECTIVES

Obtained results have emphasized the stress-strength effective nature of the contact stress in wet granular soils, as well as a limited stress-strain effective character. While possibly serving as a proxy for effective stress, the contact stress is obtained through the μUNSAT approach following general tensorial expressions, that obey the microstructure. The developements actually highlight some limitations of previous effective stress expressions, namely the absence of surface tension and a non-tensorial nature [1, 3].

While DEM provides a straightforward access to the contact stress, the μUNSAT expressions may lead to a novel way of experimentally evaluating those, by measuring the microstructure of the fluid phases using e.g. computed tomography. Indeed, comprehensive microstructure measurements would give access to the capillary stress as per Eq. (4), then to the contact stress by difference with the total stress, as per Eq. (2).

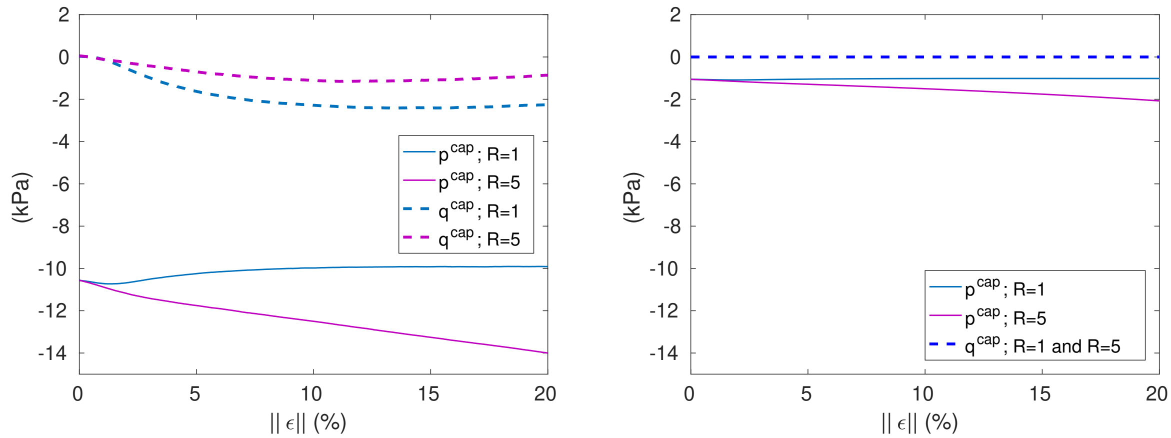

Figure 6: Capillary stresses during the two loading paths $R = 1$ and $R = 5$ imposed on the dense packing, as per μUNSAT expressions (left), compared with Bishop's estimation (right)

ACKNOWLEDGEMENTS

Part of this work has been led in collaboration with Félix Darve (Grenoble Alpes University), Mahdad Eghbalian and Mehdi Pouragha (University of Calgary).

REFERENCES

[1] N. Khalili and M. H. Khabbaz. A unique relationship for χ for the determination of the shear strength of unsaturated soils. *Géotechnique*, 48(5):681–687, 1998.

[2] N. Lu and W. Likos. Suction stress characteristic curve for unsaturated soil. *Journal of Geotechnical and Geoenvironmental Engineering*, 132(2):131–142, 2006.

[3] M. Nuth and L. Laloui. Effective stress concept in unsaturated soils: Clarification and validation of a unified framework. *International Journal for Numerical and Analytical Methods in Geomechanics*, 32(7):771–801, 2008.

[4] L. Scholtès, B. Chareyre, F. Nicot, and F. Darve. Micromechanics of granular materials with capillary effects. *International Journal of Engineering Science*, 47(1):64 – 75, 2009.

[5] R. Wan, J. Duriez, and F. Darve. A tensorial description of stresses in triphasic granular materials with interfaces. *Geomechanics for Energy and the Environment*, 4:73–87, 2015.

[6] J. Duriez and R. Wan. Contact angle mechanical influence for wet granular soils. *Acta Geotechnica*, 12(1):67–83, 2017.

[7] E.E. Alonso, J.-M. Pereira, J. Vaunat, and S. Olivella. A microstructurally based effective stress for unsaturated soils. *Géotechnique*, 60:913–925(12), 2010.

[8] J. Duriez and R. Wan. A micromechanical μUNSAT effective stress expression for stress-strain behaviour of wet granular materials. *Geomechanics for Energy and the Environment*, 15:10–18, 2018.

[9] J. Duriez, R. Wan, M. Pouragha, and F. Darve. Revisiting the existence of an effective stress for wet granular soils with micromechanics. *International Journal for Numerical and Analytical Methods in Geomechanics*, 42(8):959–978, 2018.

[10] J. Duriez and R. Wan. Stress in wet granular media with interfaces via homogenization and discrete element approaches. *Journal of Engineering Mechanics*, 142(12), 2016.

[11] J. Duriez, M. Eghbalian, R. Wan, and F. Darve. The micromechanical nature of stresses in triphasic granular media with interfaces. *Journal of the Mechanics and Physics of Solids*, 99:495–511, 2017.

[12] X. Chateau and L. Dormieux. Homogenization of a non-saturated porous medium: Hill's lemma and applications. *C. R. Acad. Sci. Paris, Série II*, 320:627–634, 1995.

[13] W. G. Gray, B. A. Schrefler, and F. Pesavento. The solid phase stress tensor in porous media mechanics and the Hill–Mandel condition. *Journal of the Mechanics and Physics of Solids*, 57(3):539 – 554, 2009.

[14] E. Nikooee, G. Habibagahi, S. M. Hassanizadeh, and A. Ghahramani. Effective stress in unsaturated soils: A thermodynamic approach based on the interfacial energy and hydromechanical coupling. *Transport in Porous Media*, 96(2):369–396, 2013.

[15] E. N. Parker. Tensor virial equations. *Phys. Rev.*, 96:1686–1689, 1954.

[16] J. Duriez, R. Wan, and M. Pouragha. Partially saturated granular materials: Insights from micro-mechanical modelling. In *Proceedings of the 6th Biot Conference on Poromechanics*, pages 441–448, 2017.

[17] J. Duriez, R. Wan, and F. Darve. Microstructural views of stresses in three-phase granular materials. In S. Bouvier D. Brancherie, P. Feissel and A. Ibrahimbegovic, editors, *From Microstructure Investigations to Multiscale Modeling: Bridging the Gap*, pages 143–165. John Wiley & Sons, Inc., 2017.

[18] A. W. Bishop and G. E. Blight. Some aspects of effective stress in saturated and partly saturated soils. *Géotechnique*, 13:177–197, 1963.